

Investigation of the Structural Stability of Nanostructured Al-5.7wt.%-Ni Mechanically Alloyed Eutectic Alloy Powders

Mohyeldin Ragab¹, Hanadi G. Salem²

¹Department of Civil and Environmental Engineering, Materials Specialization,
North Dakota State University, Fargo, ND, USA

²Department of Mechanical Engineering, The Yousef Jameel Science and Technology Research Center (YJ-STRC),
The American University in Cairo, Egypt

Keywords: Al-5.7wt.%-Ni, Eutectic Alloy, Mechanical Alloying, Structural Stability, Isothermal Heating.

Abstract

In the current research, differential scanning calorimetry (DSC), scanning electron microscopy (SEM), and transmission electron microscopy (TEM) were employed to determine the structural stability of nanostructured Al-5.7wt.%-Ni mechanically alloyed (MA) eutectic alloy powders. DSC traces were employed to determine the variation in the amount of stored energy and dislocation density as a function of milling conditions. SEM imaging was employed to investigate the degree of structural stability against grain growth as a function of the isothermal heating of MA milled powder. TEM was utilized to investigate the influence of isothermal heating on the MA nanoscale structured powders resistance to coarsening. It was found that the increasing the milling energy (RPM, ball-to-powder-ratio and time) resulted in increasing the amount of stored energy as well as increasing the dislocation density, which increased the susceptibility for grain growth.

Introduction

The utilization of aluminum alloys in aerospace applications, automobile and many other industries is widely carried out as a result of their low density and high specific strength and modulus. Improvement in hardness, rigidity and other mechanical properties as well as enhancement in the relatively low thermal properties of aluminum is achieved by utilizing alloying elements [1]. Compared to other Al-base alloys, Al-Ni alloys are known to have relatively stronger properties at relatively higher operating temperature. When moderate operating temperatures are in demand, fabrication of Al-Ni alloys with enhanced strength and stiffness at temperatures higher than room temperature could substitute for some of the Ni-base alloys. The structural stability of the fabricated alloys heavily influences the strength and creep resistance of Al-Ni alloys. This is also influenced by the initial grain size utilized in addition to the secondary phase morphologies and stability against over aging. Several industrial applications utilize the Ni-rich, Al-Ni alloys as a result of their high strength up to 800°C and their resistance to deformation, wear and fatigue. On the other hand, powder consolidation and processing via special techniques are required as a result of such alloys brittleness, large shrinkage cavities, micro-porosities, this adds to the production cost [2]. On the other hand, Al-rich, Al-Ni alloys are known for their relatively high strength at room temperature, very low porosity and hence higher densification by Powder Metallurgy (PM) and lower manufacturing costs. However, this is on the expense of their low softening temperatures compared to the Ni-rich alloys and their lower strength compared to other Al-alloys since they are non

precipitation hardenable alloys [3]. Al-5.7 wt% Ni eutectic alloy is made of fibrous eutectic microconstituent that is 86.4% α -Al solid solution, and 13.58% Al_3Ni intermetallic compound. The α -Al solid solution matrix contains a maximum of 0.05% Ni at room temperature [3]. The Al_3Ni intermetallic lamellae or platelets are known for their high hardness and strength, which provides the alloy with the necessary structural stability at operating temperatures higher than room temperature. Morphology of the eutectic structure influences significantly the produced mechanical properties.

Mechanical milling processing techniques are capable of changing the eutectic platelets into despersoids. The process of mechanical alloying (MA) involves repeated cold welding, fracturing, and re-welding of powder particles in a ball mill. MA allows the synthesis of homogeneous materials starting from blended elemental powder mixtures. Mechanical alloying is also known for its ability of extending the solid solubility beyond that produced by conventional solidification in many alloy systems by non-equilibrium processing. Ni solubility in α -Al milled MA powders was found to increase up to maximum of 10% compared to an equilibrium value of 0.1 % [4].

Refinement of the material structure to the nanoscale level has proven to enhance the mechanical properties of the bulk material due to the increased surface area of boundaries that stops motion of dislocations.

In previous work by the team, nanocrystalline Al-5.7wt% Ni eutectic alloy bulk samples were produced via MA with enhanced strength/toughness combination of properties [5]. However, the structural stability of such nanostructured eutectic alloy was not fully addressed. The aim of this work is to investigate the structural stability of the produced nanostructured eutectic alloy by determining the variation in the amount of stored energy and dislocation density as a function of milling conditions.

Materials, Processing and Characterization

Powders material

The nanocrystalline Al-5.7wt% Ni eutectic alloy powders utilized in the current work were synthesized via MA from gas atomized pure Al micron-powder (99.7% purity) and pure Ni micron-powders (99.7 % purity). The as-received Al powder particles were characterized by their non uniformity in shape and size, which ranged between 5-75 μm with an average of 45 μm . The Al micron powder had an average grain size of 3 μm . The as-received Ni powders had an ultrafine particle size which ranged from 0.5 to 6 μm in size with an average of 3 μm . The Ni powders had an average grain size of 150 nm. The detailed procedure for the processing steps was presented in detail in a previous work by this research team [5].

Mechanical Alloying

As mentioned earlier, the nanocrystalline Al-5.7wt% Ni eutectic alloy utilized in this research work was synthesized via MA from Al and Ni powders. MA of the Al-Ni powder mixture with the stoichiometric alloy composition (Al-5.7wt% Ni) was conducted in a RETSCH PM 400 high-energy planetary ball mill employing various milling conditions as listed in Table 1 [5].

Table 1 Milling parameters

BP wt. ratio	Milling Speeds(RPM)		
	200	300	350
5:1	200	300	350
10:1	200	300	350
15:1	200	300	350
20:1	200	300	350

Handling and weighting powders were conducted in a glove box under controlled atmosphere of argon gas. Milling continued for 40 hrs inside stainless steel vials of volume 125 ml with stainless steel balls of 10mm diameter. Ethanol was added as a process control agent (PCA) with 5%wt of the powder charge, to minimize cold welding between powder particles and to prevent agglomeration as stated by Suryanarayana [4]. Milling took place at interrupted intervals of 15 min to avoid overheating of the powders.

Table 2 shows the starting and completion time of the nanocrystalline Al-5.7wt% Ni eutectic alloy formation that was carried out in a previous work by this research team [5].

Table 2 Experimentally determined MTs for the eutectic alloy start and complete formation up to 40hrs [5].

RPM	Ball To Powder wt. ratio							
	5:01		10:01		15:01		20:01	
	Starting time (hr)	Completion time (hr)	Starting time (hr)	Completion time (hr)	Starting time (hr)	Completion time (hr)	Starting time (hr)	Completion time (hr)
200	UF	UF	33	UF	15	UF	11	UF
300	19	UF	10	UF	5	21	3	16
350	12	UF	6	29	4	19	2	10

UF: Eutectic alloy is unformed.

Characterization

Thermal analysis

DSC was employed for determination of the structural stability of the milled powders at the various conditions by determining the stored energy and the dislocation density induced by the various milling parameters. Powder samples with a constant mass of 35mg were examined. Powders after 40 hrs of MT were tested. Four samples from each condition were tested for results consistency. Samples were crimped using crimper provided by Perkin Elmer. Unvented aluminum sample pans and covers were used to encapsulate the powder samples. An average of the results produced from four samples per processing condition was calculated. The DSC was purged with nitrogen for 1 hour before starting each experiment. The tests were done at a rate of 10 °C/min and with the purge gas continuing during the tests. The second-run approach was employed to determine the amount of stored energy and consequently the dislocation density as shown in Figure 1 [6].

In the first run the sample was heated from 50 to 550 °C at a rate of 10 °C/min. At the end of the first run the sample was left to

cool without opening the sample cover, then the DSC was kept for 10 minutes at 25 °C to stabilize; following that the second run was started with the same procedure. The DSC curve of the second run was used to fit a baseline under the exothermic peak and between the initial and the final peak temperatures [6]. Finally, the Perkin Elmer Pyris software was used to measure the area bounded by the exothermic and the fitted baseline between the limits set by the initial and the final peak temperatures. The DSC that was employed to examine the samples was Perkin-Elmer Diamond DSC equipped with Intracooler System and Autosampler.

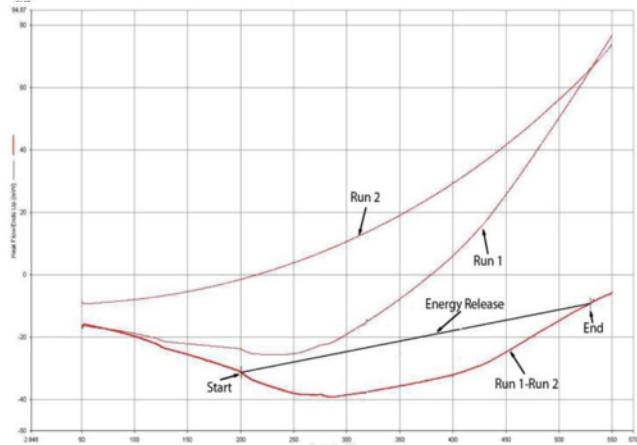


Figure 1 Second Run approach.

Determination of the amount of stored energy

The release of the stored energy can be measured as a function of temperature using DSC [7]. By employing the second run approach, where the test sample undergoes the same procedure of heating for two consecutive times to determine the baseline against the exothermic peak in the DSC curve, the stored energy within a material can be measured. When the test sample undergoes an exothermic reaction such as recrystallization, the amount of heat release appears as a peak in the DSC curve by subtracting the baseline of the second run from the first run, having the total area under the peak representing the total heat released. Owing to the fact that all the energy associated with the deformation-induced defects would have been released during the first heating run itself, the second run would provide the baseline against which the area under the exothermic peak (from the first run) can be measured.

Calculation of dislocation density

Owing to the fact that the presence of dislocations in a material is equivalent to a certain amount of stored internal energy, measurement of stored energy can thus be an indirect method for determining dislocation density. Counting the number of intersections of dislocations with a grid of lines in a transmission electron microscope (TEM) image of the material is the conventional method of measuring dislocation density in a material [8].

$$\rho = \left(\frac{N_1}{L_1} + \frac{N_2}{L_2} \right) \frac{1}{t} \quad [7]$$

Where L1 and L2 are the total length of grid lines in two mutually perpendicular directions, N1 and N2 are the corresponding number of intersections with the dislocations and t is the thickness of the foil being examined. This method can't be applied when the

individual dislocations cannot be resolved (e.g. due to a large dislocation density) [7].

When a deformed material is heated to a sufficiently high temperature, it releases energy while undergoing recovery (dislocation rearrangement) and possibly, recrystallization (dislocation annihilation). The amount of stored energy is the area bounded by the exotherm and the fitted baseline between the limits set by the initial and the final peak temperatures [6]. Based on the dislocation theory, the dislocation density is related to the dislocation-stored energy (E) such that [9]:

$$E = \rho \frac{Gb^2 f(\nu)}{4\pi} \ln \left(\frac{R}{R_o} \right) \quad [9]$$

Where R is the inner radius of the dislocation core (taken between b and 5b), R_o is the outer radius (taken as the inter-dislocation core spacing, ρ^{1/2}), and f(ν) is a function of Poisson's ratio f(ν) = (1-ν/2)/(1-ν), considering both screw and edge dislocations.

The previous expression is commonly replaced by an approximate expression from which the calculation of dislocation density from DSC curves can be utilized, using the equation [9]:

$$E = \alpha \rho G b^2 \quad [10]$$

Where E is the amount of stored energy obtained from the DSC curve, α is the dislocation interaction parameter that is of the order of 0.5, G is the shear modulus and b is the burgers vector [10].

Scanning Electron Microscopy

Powders morphology and structural evolution were investigated by Scanning Electron Microscopy (SEM) imaging of the as-milled powders before and after isothermal heating (IH). A 200kV Leo Zeiss field emission scanning electron microscope with resolution of 1.0nm was employed in the current research. SEM micrographs for nanocrystalline Al-5.7wt% Ni eutectic alloy powders synthesized under 20:1 BPR and 300 RPM at alloy completion time (16hrs) and after 40hrs of MT were taken before and after IH.

Transmission Electron Microscopy

The Transmission Electron Microscopy (TEM) images were employed for the investigation of the internal nanostructure of the milled Al-Ni eutectic powders before and after IH. In addition, TEM images were used to evaluate the eutectic structure morphology evolution at the alloy formation time and after 40hrs of MT. The analysis was completed using a JEOL 2010 TEM operated at 200kV with a spatial resolution of 1.9 Angstrom. TEM images for nanocrystalline Al-5.7wt% Ni eutectic alloy powders synthesized under 20:1 BPR and 300 RPM at alloy completion time (16hrs) and after 40hrs of MT were taken before and after IH.

Results and Discussions

Thermal Analysis

Variation of Stored Energy with milling parameters

Figure 2 illustrates the variation of stored energies measured with the various milling parameters. It can be seen that combined increase in BPR, RPM (high milling energy) resulted in increasing the amount of stored energy. At 10:1 BPR, the utilization of 300 RPM resulted in a stored energy of 7.22 Joules/g. On the other hand, the utilization of 350 RPM led to a stored energy of 9.15 Joules/g. Increasing the BPR to 15:1 led to an increase of the

stored energy for both RPM employed. At a combination of 15:1 BBR and 300 RPM, the stored energy was 12.65 Joules/g. While upon utilizing 15:1 BBR and 350 RPM, the stored energy was 14.82 Joules/g. The combination of 20:1 BPR and 300 RPM resulted in a stored energy of 16.19 Joules/g. Increasing the RPM to 350 with the same BPR (20:1) yielded a stored energy of 18.03 Joules/g.

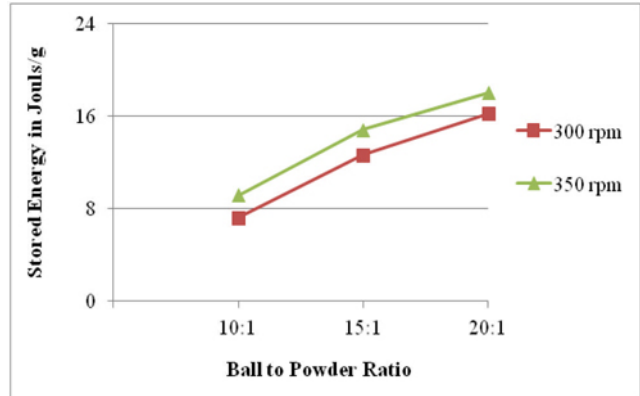


Figure 2 Variation of stored energy with milling parameters at 40 hrs MT

Variation of dislocation density with milling parameters

Figure 3 shows the variation of the dislocation density for the various combination of BBR and RPM. Similar behavior for the stored energy can be seen for dislocation density.

The combined increase in BPR and RPM (high milling energy) resulted in increasing the amount of dislocation density. At 10:1 BPR, the utilization of 300 RPM resulted in a dislocation density of 2.86X10¹⁶ disl./m². On the other hand, the utilization of 350 RPM led to a dislocation density of 3.74X10¹⁶ disl./m². Increasing the BPR to 15:1 led to an increase of the dislocation density for both RPM employed. At a combination of 15:1 BBR and 300 RPM, dislocation density was 5.01X10¹⁶ disl./m². While upon utilizing 15:1 BBR and 350 RPM, the dislocation density was 5.87X10¹⁶ disl./m². The combination of 20:1 BPR and 300 RPM resulted in a dislocation density of 6.42 X10¹⁶ disl./m². Increasing the RPM to 350 with the same BPR (20:1) yielded a stored energy of 7.25 X10¹⁶ disl./m².

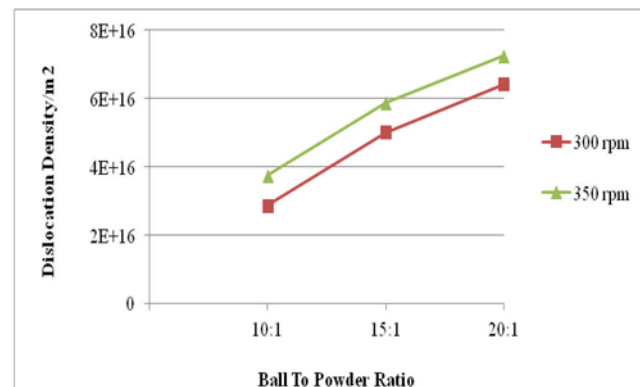


Figure 3 Variation of dislocation density with milling parameters at 40 hrs MT

Although, the dislocation densities calculated for a number of the conditions examined in this research were in the order of 10¹⁶ for the higher BPR and RPM (high milling energy), yet this agrees

with Révész *et al.*, who reported similar results as a result of longed milling durations[11]. In addition, Godfrey *et al.*, reported that the stored energies calculated from DSC curves are always exaggerated from that obtained based on the microstructural investigations [1].

Structural stability of milled powders

SEM micrographs

To investigate the degree of structural stability against grain growth, IH of the Al-5.7%wt Ni MA eutectic alloy powders at alloy completion and 40 hrs of MT at 500°C (sintering temperature) were investigated over a duration of 1 hr. IH was conducted for the eutectic alloy powders that formalized from the milling of Al and Ni powders with the utilization of 300 RPM and 20:1 BPR at 16 (representing the alloy completion time for this condition) and 40 hrs of MT, based on our previous work [5]. Figure 4 shows the internal structure of powders milled at 16 hrs.

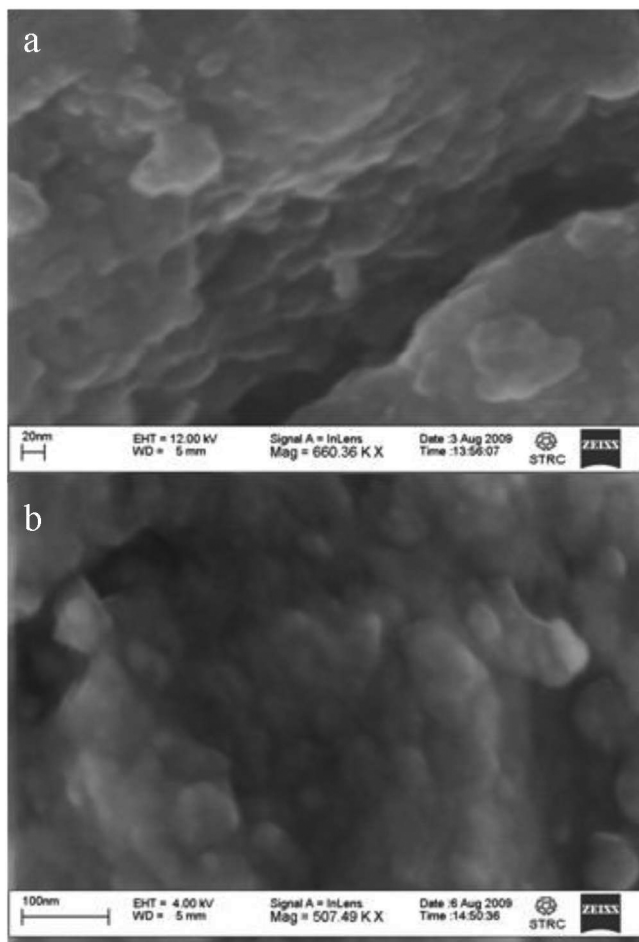


Figure 4 SEM micrograph for 20:1 BPR, 300 RPM at 16hrs MT (a) Before IH (b) After IH

The SEM images revealed the formation of grains with 20nm in average size, as illustrated in Figure 4(a). IH resulted in slight coarsening of the milled powder structure up to 25nm as shown in Figure 4(b).

Figure 5(a) shows the internal structure of the eutectic alloy powders milled at 40 hrs MT. The SEM images revealed the formation of grains with 14nm in average size. IH resulted in

slight coarsening of the milled powder structure up to 20nm as shown in Figure 5(b).

It is clear that the % grain coarsening induced by IH of the eutectic alloy powders milled at 16 hrs MT was 25 % compared to 53 % for the 40 hrs MT, which indicates higher thermal stability for the powders exposed to lower milling energy. It is suggested that the higher stored energy induced by milling (high ρ of dislocation and finer structure) increased the tendency of the powders for grain growth.

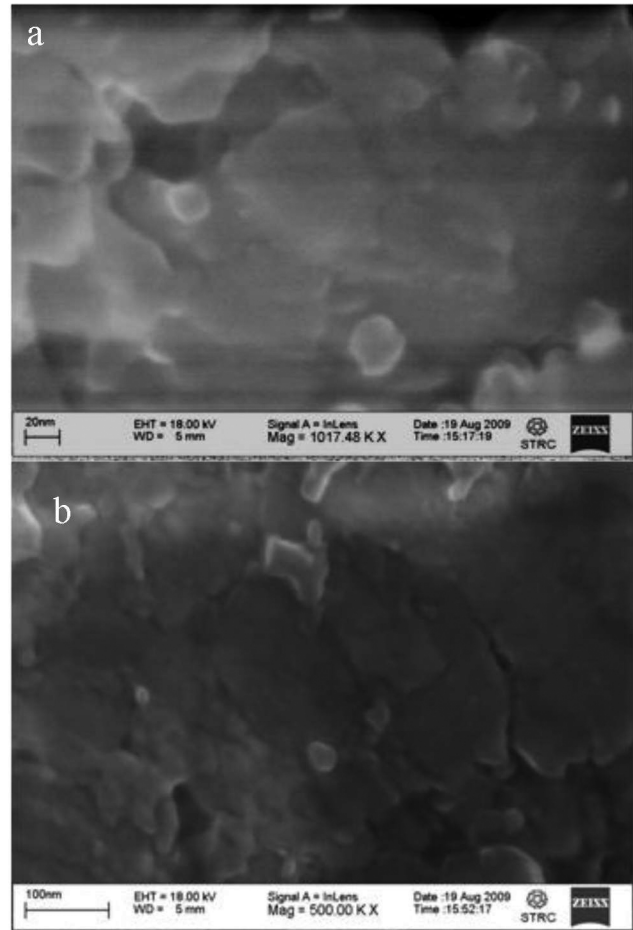


Figure 5 SEM micrograph for 20:1 BPR, 300 RPM at 40 hrs MT (a) Before IH (b) After IH

TEM images

The internal structure of the eutectic alloy powders milled at 20:1 BPR, 300 RPM for 16 hrs before and after IH is shown in Figure 6 (a) and (b) respectively. The images revealed finer structure for the as milled powders compared to that obtained after IH. An average grain size of 18.5 and 27.3 nm were measured for the eutectic alloy powders milled for 16 hrs MT before and after IH, respectively. While for the eutectic alloy powders milled for 40 hrs illustrated in Figure 7 (a) and (b), average grain sizes of 15.2 and 25nm were measured before and after IH, respectively.

It is clear that the % grain coarsening induced by IH of the alloy powders milled at 16 hrs MT was 47.17 % compared to 64.4 % for the 40 hrs MT, which indicates higher thermal stability for the powders exposed to lower milling energy. As explained earlier in the SEM results, it is suggested that the higher stored energy

induced by milling (high ρ of dislocation and finer structure) increased the tendency of the powders for grain growth.

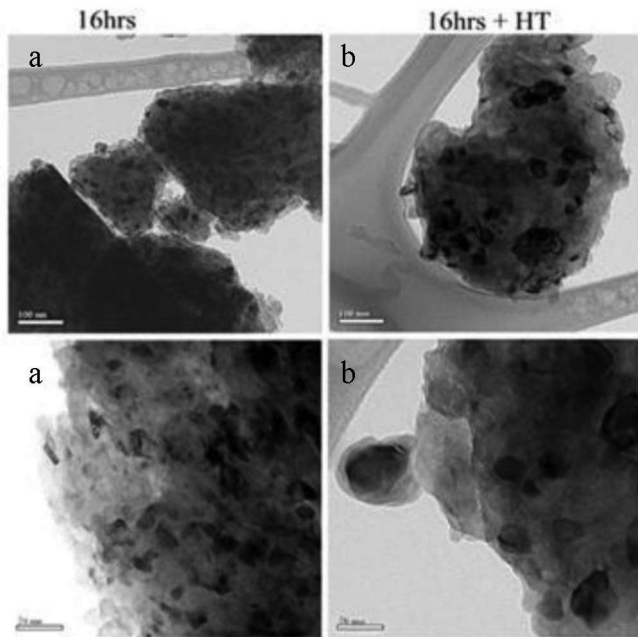


Figure 6 TEM images for eutectic alloy powders at 20:1 BPR, 300 RPM (a)Before IH and (b)After IH at 16 hrs MT.

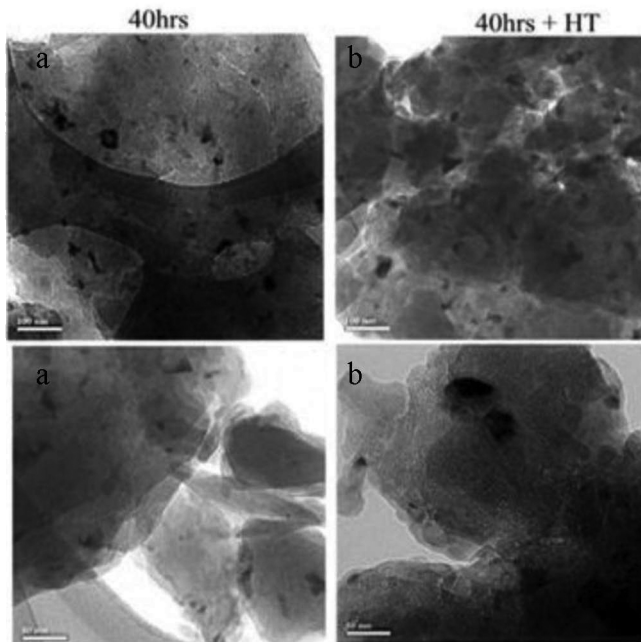


Figure 7 TEM images for eutectic alloy powders at 20:1 BPR, 300 RPM (a)Before IH and (b)After IH at 40 hrs MT.

Conclusions

1. Increasing either the milling BPR or RPM increases the amount of stored energy via strain hardening of the eutectic alloy milled powders at the same MT.
2. Stability of milled powders internal nanostructure is retained even after isothermal heating.
3. The eutectic alloy MA powders at the 16 hrs of milling displays the highest structural stability against grain growth compared to the 40 hrs milled compacts powders.
4. The higher the stored energy via high energy ball milling the higher the tendency for grain growth and hence the eventual loss of the nanostructure.

References

1. Ghomashchi M, R., "Fabrication of near net-shaped Al-based intermetallics matrix composites", *J Mater. Process. Technol.*, (2001), 112, pp: 227-235.
2. Pope D, P, Ezz S, S., "Mechanical properties of Ni3Al and nickel-base alloys with high volume fraction of γ' ", *Int. J. Met.*, (1984), 23, pp: 136-167.
3. Rohatgi P, K, and Prabhakar K, V., "Wrought Aluminum-Nickel Alloys for High Strength-High Conductivity Applications", *Metallurgical Transactions A*, (1975), 6a, pp.:1003-1008.
4. Suryanarayana C., "Nanocrystalline materials", *Inter. Mater. Rev.*, (1995), 40, pp.: 41-64.
5. Ragab, MohyEldin, and Hanadi G. Salem. "Effect of milling energy on the structural evolution and stability of nanostructured Al-5.7 wt.% Ni mechanically alloyed eutectic alloy." *Powder Technology* 222 (2012): 108-116.
6. Rohatgi A., Vecchio K.S., "The variation of dislocation density as a function of the stacking fault energy in shock-deformed FCC materials", *Materials Science and Engineering*, (2002), A328, pp.: 256-266.
7. www.dur.ac.uk/n.r.cameron/Assets/Group%20talks/DSC%20presentation.ppt (8/12/2014)
8. Plato C. and Glasgow S.R., Jr., *Anal. Chem.*, (1969), 41, pp.: 330
9. Honeycombe R, W, K., "The Plastic Deformation of Metals", 2nd ed. London: Edward Arnold, 1984.
10. Humphreys F, J, and Hatherly M., "Recrystallization and Related Annealing Phenomena", (1995), Great Britain: Pergamon,
11. Révész A., Ungár T., Borbély A, and Lendvai J., "Dislocations And Grain Size In Ball-Milled Iron Powder", *Nanostructured Materials.*, (1996), 7, No. 1, pp.: 779-788.
12. Godfrey A., Liu Q., "Stored energy and structure in top-down processed nanostructured metals", *Scripta Materiala*, (2009), 60, pp.:1050-1055